X-693-71-64
PREPRINT

NASA TM X- 65616

THE RADIO ASTRONOMY EXPLORER SATELLITE A LOW FREQUENCY OBSERVATORY

R. R. WEBER
J. K. ALEXANDER
R. G. STONE

JUNE 1971

GSFC
GODDARD SPACE FLIGHT CENTER
GREENBELT, MARYLAND

THE RADIO ASTRONOMY EXPLORER SATELLITE

A LOW FREQUENCY OBSERVATORY

by

R. R. Weber, J. K. Alexander, R.G. Stone
Radio Astronomy Branch
Laboratory for Extraterrestrial Physics
NASA/Goddard Space Flight Center
Greenbelt, Maryland

ABSTRACT

The Radio Astronomy Explorer Satellite (RAE-1) is the first spacecraft designed exclusively for radio astronomical studies. It is a small, but relatively complex, observatory including two 229-m antennas, several radiometer systems covering a frequency range of 0.2 to 9.2 MHz, and a variety of supporting experiments such as antenna impedance probes and TV cameras to monitor antenna shape. Since its launch in July, 1968, RAE-1 has sent back some 10^{10} data bits per year on measurements of long-wavelength radio phenomena in the magnetosphere, the solar corona, and the galaxy. In this paper we describe the design, calibration, and performance of the RAE-1 experiments in detail.

To appear in Radio Science

I. HISTORY

The potentialities of artificial earth satellites for radio astronomy were quickly recognized and enumerated when space research was still in its infancy (see, for example Getmantsev, et al. 1958; Lovell, 1959; and Haddock, 1960). The first low-frequency measurements of the cosmic noise background intensity from above the ionosphere were obtained by Canadian investigators (Chapman and Molozzi, 1961) using a satellite-borne receiver in 1960. A number of experiments followed on sounding rockets (Walsh et al., 1964; Huguenin et al., 1964) and on the satellites Alcuette-1 (Hartz, 1964a), Ariel-2 (Smith, 1965), and Elektron-2 (Benediktov et al., 1965). As was noted by F.G. Smith (1964), their observations sometimes tended to be "geophysical rather than astronomical". Nevertheless, these early measurements provided an important basis for further radio astronomical measurements in the upper ionosphere by isolating such problems as the perturbations to antenna impedance and radio propagation conditions arising from the ionospheric plasma.

By the mid 1960's, groups in the U.S., Canada, Great Britain, France and the U.S.S.R. had conducted a number of experiments on satellites and sounding rockets. The average cosmic noise background spectrum had been measured down to

around 1 MHz (with an absolute uncertainty of nearly ± 3 db) providing confirmation of the ground-based observations of Ellis and co-workers (Ellis et al., 1962) that the spectrum peaked at a few MHz and then fell off at lower frequencies due to absorption by galactic ionized hydrogen. Type III solar radio bursts observed near 1 MHz had provided a means of studying coronal streamers at altitudes of the order of 10 solar radii (Hartz, 1964b). A number of intense and unexpected noise sources had been observed below 1 MHz (Huguenin and Papagiannis, 1965; Benediktov et al., 1965; Slysh, 1965), but the nature of their origin remained largely undetermined.

The concept of a satellite specifically designed for radio astronomical measurements was first investigated at the Goddard Space Flight Center in 1962, and full scale design studies were under way about two years later (Alexander and Stone, 1964). The evolution of the RAE design was influenced to a great extent by the experience gained from early sounding rocket and satellite radio measurements by the small but active community of space radio astronomy groups. For example, the techniques developed for detection and reduction of spacecraft radio frequency interference by experimenters at the University of Michigan, Harvard College

Observatory, and the Canadian Defence Research Telecommunications Establishment provided the foundation for the RAE interference control program, and the concept of a homodyne or zero-IF receiver used by the Mullard Radio Astronomy Observatory experimenters on Ariel-2 was applied to the RAE radiometer design. To meet the requirements for high absolute accuracy for radio astronomical measurements, considerable efforts were directed toward the development of the best possible instruments and techniques to obtain and maintain good calibration of the satellite radiometer systems. This development work, including experiments on five sounding rocket flights by the Goddard Space Flight Center radio astronomy group, culminated in the successful launching of RAE-1 on July 4, 1968. A summary of some key parameters of the spacecraft is given in Table 1.

II. DESIGN CONSIDERATIONS

An examination of the difficulties encountered by early experiments attempting to observe long wavelength radio emission revealed three basic problem areas. These were radio frequency interference (RFI) produced by spacecraft systems, the influence of the plasma environment on radio propagation and antenna characteristics, and the difficulties associated with deploying directive antennas in space. Special attention was given to these problems as the RAE concept evolved.

Numerous precautions were taken during the design and

TABLE 1. KEY PARAMETERS OF THE RAE-1 SATELLITE

Spacecraft

Mass	193 kg
Average power consumption	25 w

Antennas

two 229-meter traveling-V's for experiments

one 37-meter electric dipole for experiments

one 137 MHz telemetry turnstile

Experiments

four step-frequency Ryle-Vonberg radiometers operating from 0.45 to 9.18 MHz

two multi-channel total power radiometers operating from 0.2 to 5.4 MHz

one step-frequency V antenna impedance probe operating from 0.24 to 7.86 MHz

One dipole antenna capacitance probe operating from 0.25 to 2.2 MHz

Orbit

altitude	5850 km
eccentricity	<0.001
inclination	121^{o}
precession rate	0.52 degree/day

testing of the RAE spacecraft to eliminate all known or potential sources of RFI. As each electronic subsystem was delivered for integration into the spacecraft, it was tested individually and in operation with other spacecraft systems. Any unit that generated detectable RFI in the experiment frequency range was returned to the system designer for modifications. Most subsystem packages had RFI filters on all input and output leads. All subsystem packages were enclosed in continuous, shielded enclosures consisting of gold-flashed aluminum walls. The surfaces of the spacecraft aluminum honeycomb instrument shelf were also gold-flashed to provide good ground connections between all packages and the shelf. In most subsystems instrument cases were used only for shielding and not for signal grounds. Instead, separate ground returns were used for power grounds, switching grounds, logic grounds, and signal grounds. All ground leads were held to the shortest possible length. Shielded cables were used for all wires exterior to the spacecraft, all signals at a frequency of 100 Hz or above, and all signals with rise times less than 10 μs. All RF signals were carried on coaxial cables. The spacecraft outer shell was designed to provide good ground contact at all points on the shell interior and wire mesh gaskets were used to seal

all apertures in the shell. As a consequence there were no radiation paths between the outside and the inside of the spacecraft. Special filters were used to prevent signals at the telemetry frequency (136 MHz) from getting outside the spacecraft via solar panel leads or from getting into the spacecraft on experiment antenna cables. Since harmonics of the switching waveforms in dc-dc power converters had been a source of RFI problems on earlier satellites, converters that incorporated filtering and low switching frequencies were designed. As a result of these many precautions and the general recognition of the need for RFI suppression, there were no detectable interference sources above the experiment radiometer threshold levels ($\sim$ -120 dbm) before or after launch.

The orbit chosen for RAE-1 was a compromise between the need for reduced plasma effects at high altitudes and the requirement for sufficient gravitational force to provide gravity-gradient stabilization of the long antenna booms. The orbit was also limited by the capability of available launch vehicles. At the altitude of 6000 km selected as optimum, observations of extraterrestrial radio noise can often be made down to a frequency of 600 kHz over the equator and as low as 200 kHz in regions of low electron density at high latitudes. Since sky coverage is obtained

on RAE through a combination of orbital scanning and precession of the orbital plane, both high inclination and high precession rates are desirable. An orbit which provided for the longest possible time in a 100% sunlight condition was also required since the thermal shock on the long booms caused by passing into the earth's shadow was an area of some uncertainty. The optimum orbital inclination of 59^{o} retrograde provided for full coverage of 80% of the sky in less than one year and for six months of operation before any portion of the orbit was in shadow.

As a design goal for the first Radio Astronomy Explorer we sought an antenna which could provide an order of magnitude better resolution than a dipole at a number of frequencies below 10 MHz. This objective set the minimum length of the antenna at approximately 300 meters. These long antennas would have to be stored, deployed and stabilized in the space environment, and this meant mechanically weak structures which would be very flexible. As the satellite moved in its orbit, the antenna would be subjected to variable driving forces arising from changes in solar illumination and gravitational forces. Since such a structure would tend to be distorted from its preferred shape, an antenna would have to be found which could still function well under such distortions. For simplicity, the structure would also have to be radially deployed from the spacecraft.

III. RAE ANTENNAS

The antenna configuration chosen for RAE is shown in Figure 1. Two 229-m traveling-wave V antennas are aligned back-to-back and a 37-m dipole bisects the axis of the V's. All three antennas lie in the same plane. The traveling-wave V antenna combines the advantages of the V antenna and the traveling-wave dipole to achieve a simple structure, broad bandwidth and good directivity. The RAE V antenna full beam, consisting of the central lobe and major sidelobes, typically includes one steradian in the frequency range of 3 to 10 MHz. Each leg of the V antenna is cut one quarter of the way from its tip and a 600-ohm series resistor is inserted. The V operates as a traveling-wave antenna at frequencies where the antenna length beyond the resistor equals an odd number of quarter wavelengths. The backward response is thereby suppressed, and a front-to-back ratio of better than 10 db is achieved.

Since the interpretation of the cosmic noise background maps depends critically on our knowledge of the properties and performance of the V antenna and since there was relatively little information about this antenna in the technical literature when RAE was being designed, a number of theoretical and experimental investigations were made of its electrical and mechanical behavior. Several theoretical

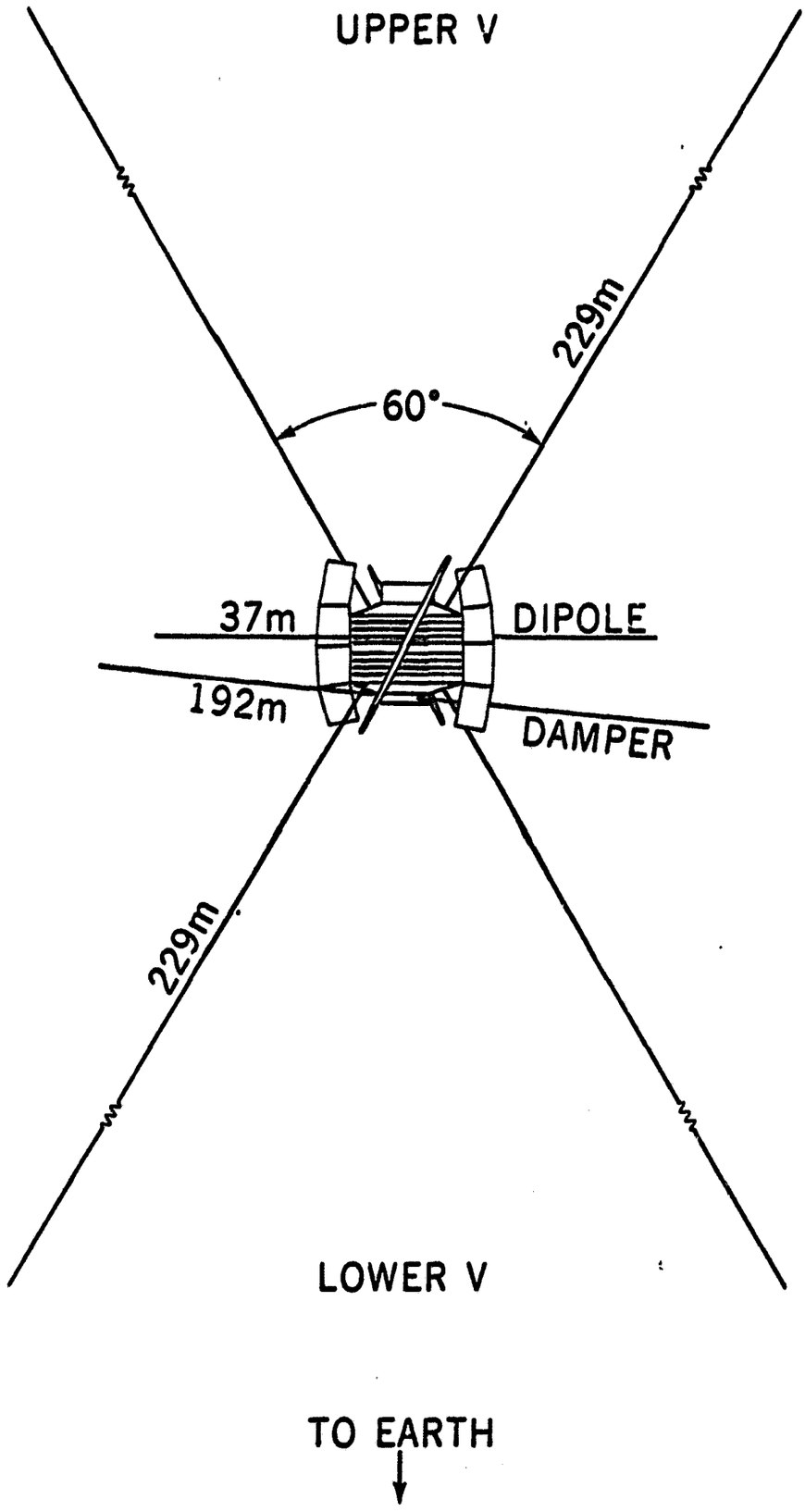

Figure 1. Diagram of the RAE-1 Antenna Boom Systems.

studies of the radiation properties of the traveling-wave V were conducted (Duff, 1964; Iizuka, 1965; Sandler, 1966), and experimental measurements were performed on models with scale factors of ~ 100:1 or greater (Iizuka, 1967). Although these scale model measurements served to confirm the theoretical treatments and to provide a basis for understanding the effects of antenna geometry and deformation on the radiation properties, the effects of element conductivity could not be scaled. Consequently a series of impedance and current distribution measurements were made by Collins Radio Co. using 4.5:1 and 3.25:1 scale models erected over a 183-m diameter ground plane. Using appropriate wire to scale the conductor size, accurate measurements of the impedance and current distribution of a single wire with its image in the ground plane were obtained. From these data, antenna patterns were calculated for a wide range of frequencies and antenna shapes. Examples of the antenna radiation patterns are shown in Figure 2. The properties of the antenna patterns determined from the Collins Radio measurements are summarized in Table 2.

A direct measure of the V antenna front-to-back ratio can be made from simultaneous measurements by both the upper and lower V's of intense noise generated in the magnetosphere

RAE V ANTENNA PATTERNS

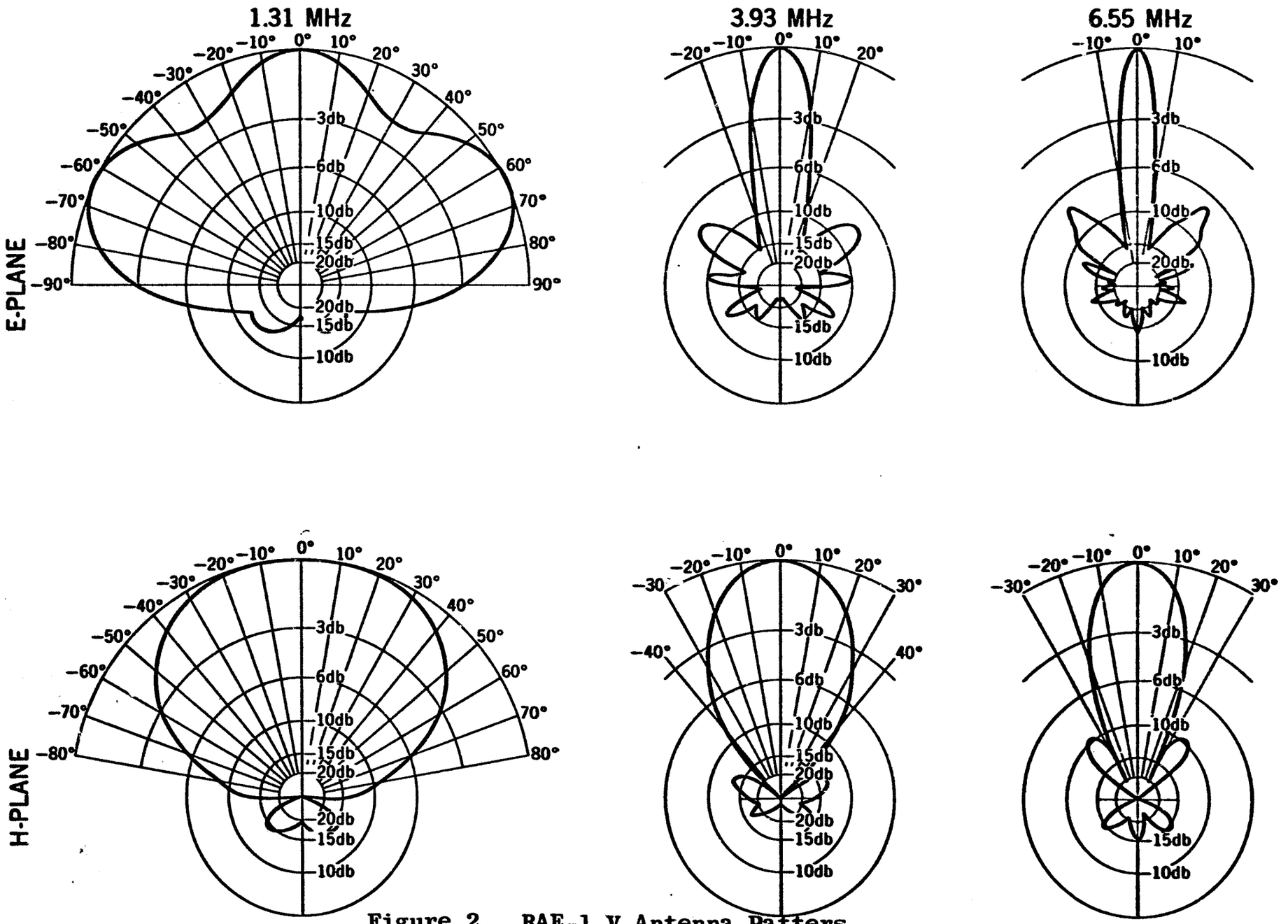

Figure 2. RAE-1 V Antenna Patters

TABLE 2. PROPERTIES OF THE RAE TRAVELING-WAVE V.

Frequency	Nominal Beamwidth	1st Side-Lobe	Front/Back Ratio	Free Space Impedance
1.31 MHz	180 degrees	-	12 db	335-j 120 ohms
2.20	44 x 84	-3 db	4	120-j 180
3.93	23 x 52	-7	13	380-j 90
4.70	15 x 46	-5	6	260-j 340
6.55	14 x 34	-7	15	340-j 50
9.18	13 x 27	-5	13	340-j 60

below the satellite. Figure 3 shows eight hours of data for the upper and lower V's at 3.93 MHz. The increases centered on $17^h\ 40^m$ and $21^h 20^m$ are clearly due to noise generated below the satellite. If the data are plotted as upper V antenna temperature versus lower V antenna temperature with time as a parameter, the average front-to-back ratio can be determined. The data in Figure 4 show that the front-to-back ratio of the RAE V antenna is approximately 13 db at 3.93 MHz.

The flight antenna elements are formed from 0.005-cm thick, 5-cm wide, heat-treated beryllium-copper alloy tapes which were stored on a spool in the spacecraft during launch, When deployed by a motorized mechanism, the elements form 1.3-cm diameter, hollow cylindrical tubes. Tabs along the edges of the tape interlock at the seam to provide good torsional rigidity. Since one of the primary causes of bending of the antenna elements in orbit is the thermal gradient across the boom due to sunlight illuminating only one side, special efforts were made to minimize this thermal gradient. This was done by perforating the tapes and using a polished silver plating on the outside and a black coating on the inside.

The satellite makes use of gravitational forces to keep one V pointing toward the earth and the other toward

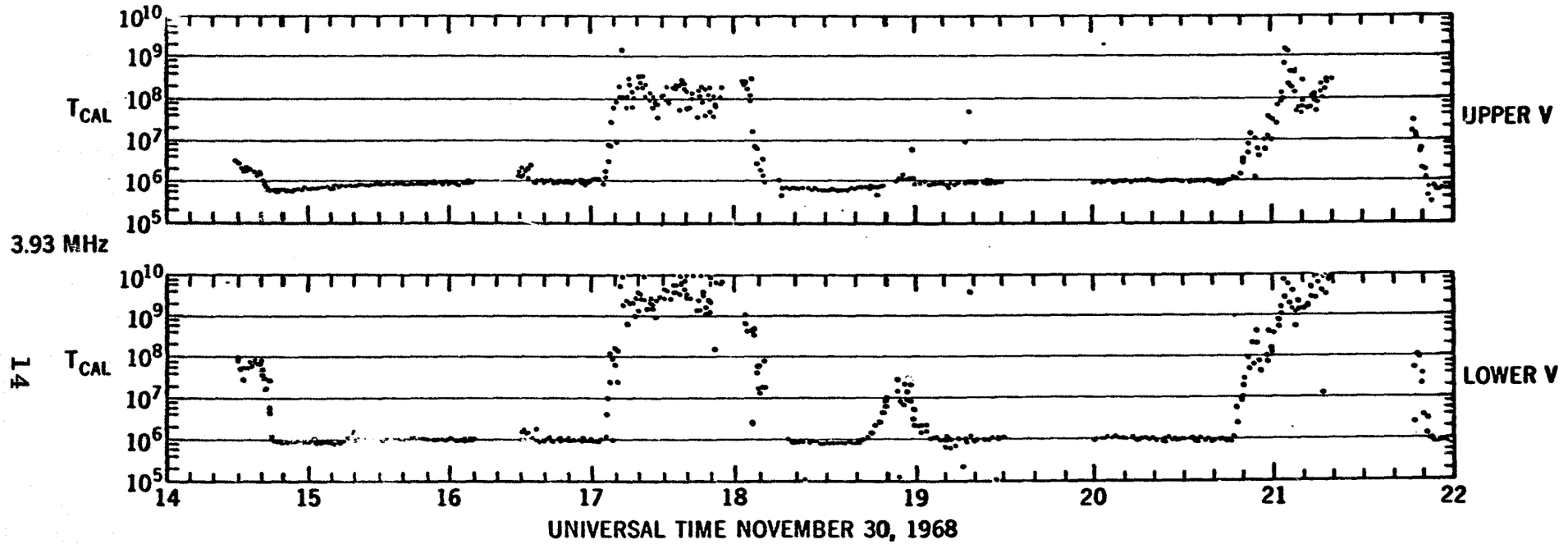

Figure 3. Sample of two orbits of V Antenna Data at 3.93 MHz Showing Periods of Intense Noise Coming from Below the Satellite. T_{CAL} is Equivalent Noise Temperature (^{o}K) at Radiometer Input.

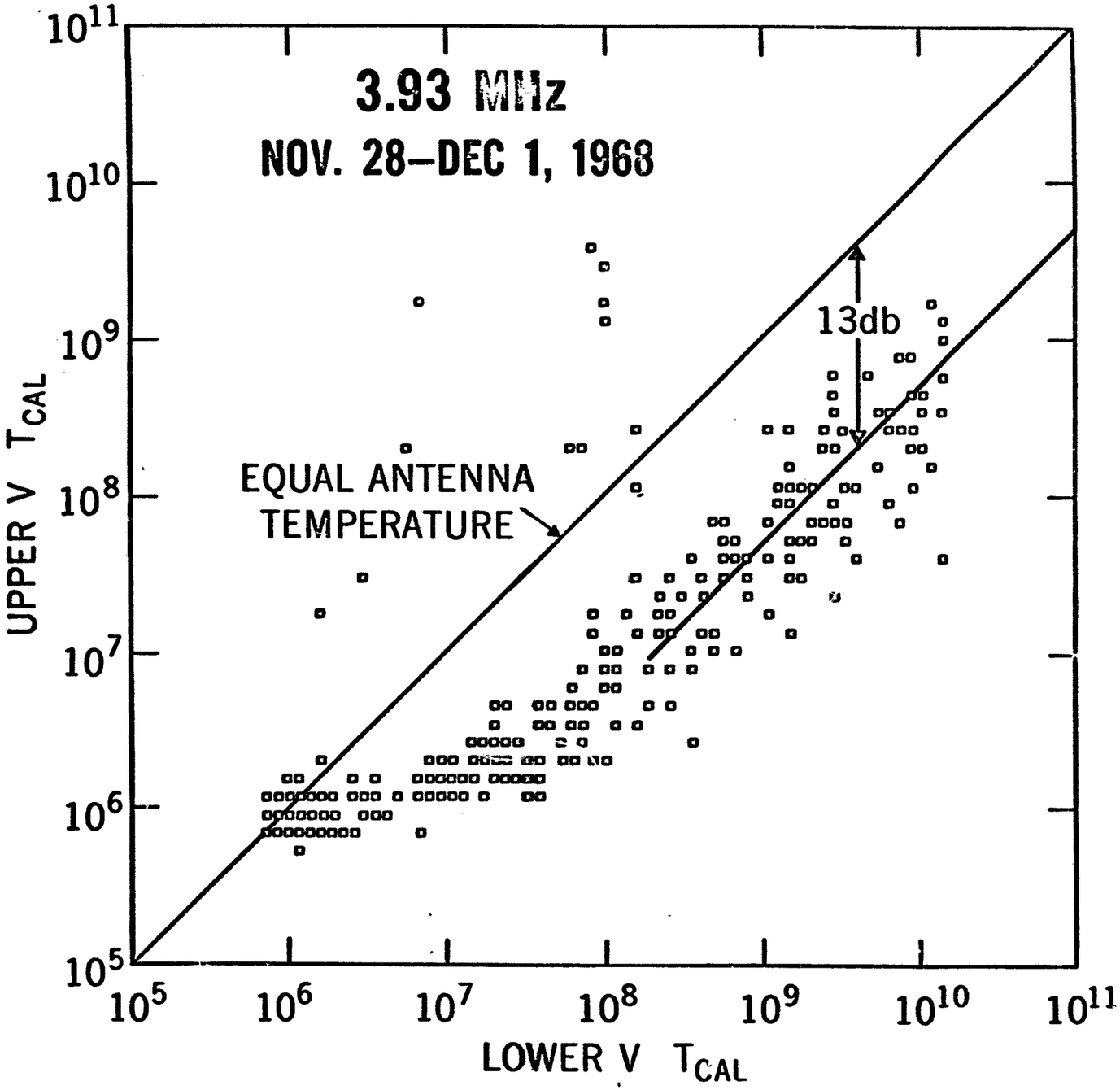

Figure 4. Plot of Upper V vs Lower V Noise Temperatures at 3.93 MHz used to determine front-to-back Ratio.

the local zenith. The gravity-gradient stabilization results from stronger gravitational attraction of the earth for the lower V than for the upper V. Gyroscopic forces hold the plane of the antennas in the orbital plane. During each orbit, the upper V scans a great circle on the celestial sphere between declination limits of $\pm 59^{\circ}$, determined by the orbital inclination. This scan then precesses with the orbital plane at a rate of 0.52° per day. As a result of the nearly circular orbit (eccentricity $\lesssim .001$) which minimizes periodic variations in gravitational forces, the oscillations of the spacecraft central body around its nominal orientation are less than $\pm 3^{\circ}$ in all three axes. A 192-meter libration damper boom in the plane normal to the major axis of the V's is suspended from the spacecraft by a torsion wire to damp out oscillations of the satellite about its equilibrium position. Two television cameras on RAE can be commanded to monitor the position of the booms relative to the central body and to each other. Tip deflections have been found to reach a maximum of about 10% of the antenna length. This is acceptable since the resultant changes in the antenna radiation patterns are small compared to the angular resolution of the antenna.

The dipole antenna is formed by two monopoles made of the same silver-coated beryllium-copper material as the

V's. Since the electrical characteristics of a simple dipole are much better understood theoretically, data from the RAE dipole have provided the basis for absolute sky brightness measurements. Inflight measurements of the dipole capacitance at frequencies between 600 kHz and 2 MHz at times when the ionospheric electron density is known to be very low have yielded values which are within a few percent of theoretical calculations. A comparison of the capacitance probe flight measurements with calculations according to the formulae of Schelkenoff and Friis (1952) and King and Middleton (King, 1956) for dipole capacitance is given in Table 3. Also given in the table are the results of theoretical calculations performed for the RAE dipole with and without the other long spacecraft booms. These calculations, carried out by Technology for Communications International, Inc., apply numerical techniques developed by Tanner and Andreasen (1967) to derive the current distributions on the booms from integral equations. The extremely close agreement between the measured capacitance and the calculated values for the satellite dipole may be fortuitous, but the results still reinforce our confidence that when ionospheric electron densities are low the dipole impedance can be determined reliably.

IV. INSTRUMENTATION

The spacecraft is equipped with three types of radiometers

TABLE 3. RAE DIPOLE FREE SPACE CAPACITANCE

Frequency	Schelkenoff and Friis	King and Middleton	TCI (dipole only)	TCI (with other booms)	Capacitance Probe
0.615 MHz	73.9 pf	74 pf	74 pf	76 pf	76 pf
0.873	75.6	76	75	78	79
1.929	92.2	92	89	94	94

and two types of impedance probes as shown in the system block diagram in Figure 5. Ryle-Vonberg radiometers are used on all three antennas to provide high accuracy and long-term stability. Fixed-frequency total-power radiometers with rapid time response are used on the dipole and lower V to monitor bursts from the sun, earth, or other sources of transient phenomena. A sweeping burst radiometer on the dipole is stepped rapidly through 32 discrete frequencies between 0.2 and 5.4 MHz to generate dynamic spectra. An impedance probe periodically measures the complex impedance of each V antenna, and a capacitance probe measures the capacitance of the dipole antenna.

A Ryle-Vonberg feedback radiometer design was used on RAE because its insensitivity to gain and bandwidth changes provides the stability necessary for the sky mapping over many months of operation. A block diagram of the satellite radiometer system developed at the Goddard Space Flight Center (Somerlock and Krustins, 1968), is shown in Figure 6. A Dicke switch driven by a 100 Hz oscillator continuously switches the radiometer input between the antenna and a calibrated voltage-controlled noise source. The RF section of the radiometer consists of nine separate tuned RF input amplifiers having a bandwidth of 200 kHz, a wide band amplifier,

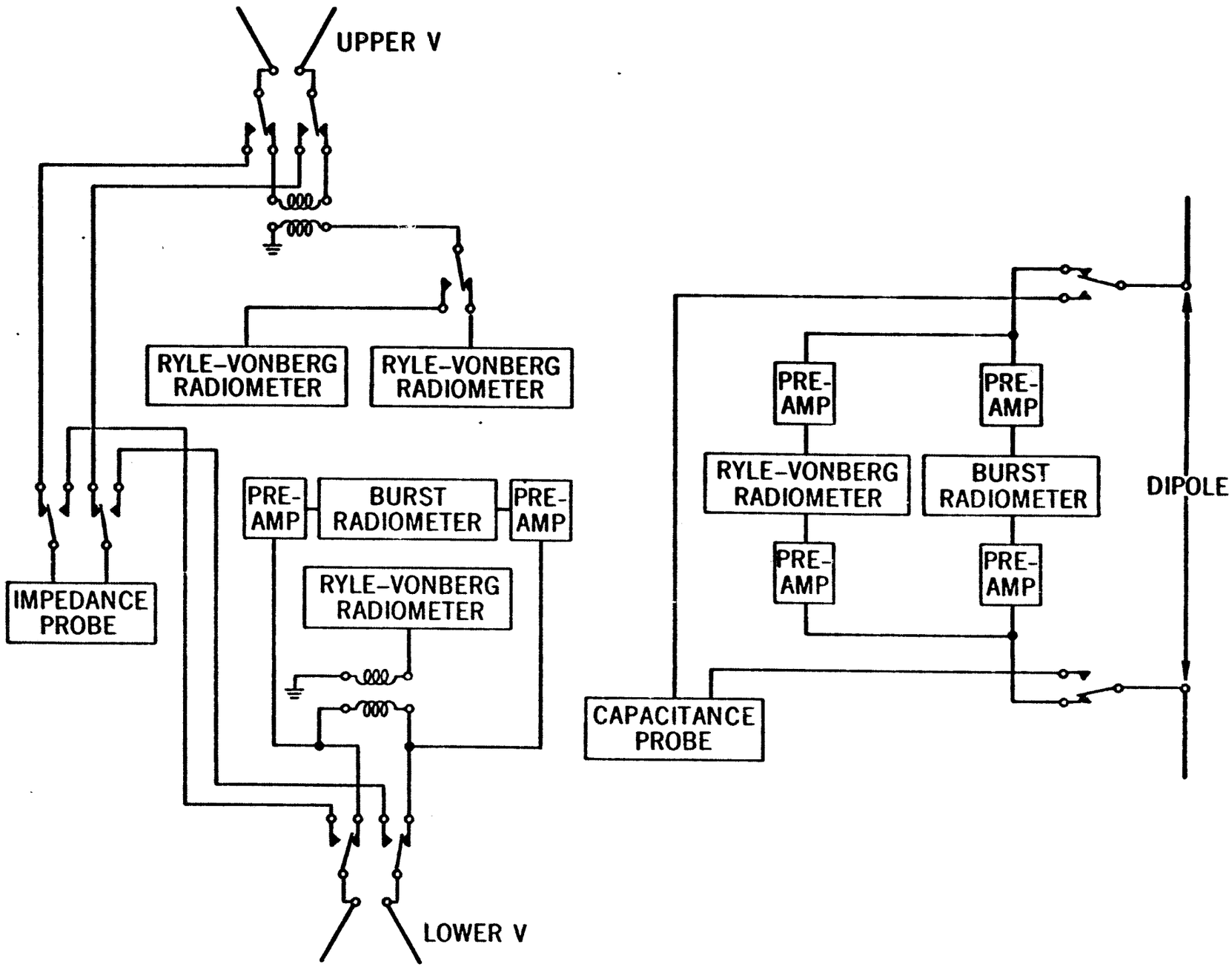

Figure 5. Simplified Block Diagram of RAE-1 Experiment Systems.

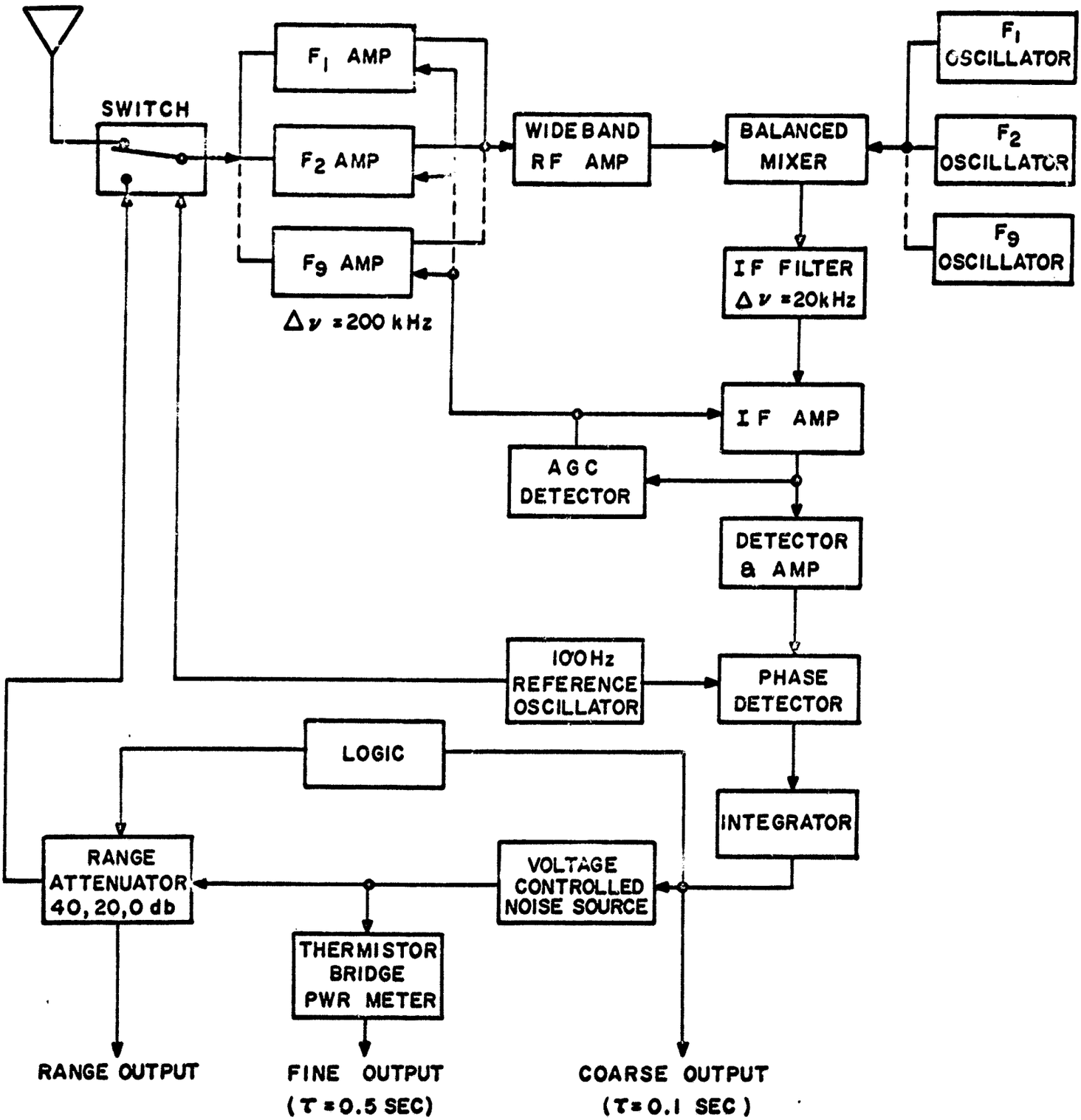

Figure 6. Block Diagram of Ryle-Vonberg Radiometer

a balanced mixer, and an IF filter and amplifier. The RF input amplifiers operate at 0.45, 0.70, 0.90, 1.31, 2.20, 3.93, 4.70, 6.55 and 9.18 MHz, and they are turned on individually in a sequence that steps the radiometer through all nine channels every 72 seconds. Nine separate crystal local oscillators are stepped in synchronism with the RF amplifiers. Separate local oscillators and RF amplifiers tuned to the same frequency were used to provide a relatively narrow input bandwidth and high system reliability. The mixer output which contains the difference frequencies between the local oscillator and the RF noise input in the 1 Hz to 100 kHz range is then passed through a 10-to-30 kHz bandpass IF filter. This "zero - IF" technique eliminates image problems by using the image as part of the signal, providing an effective RF bandwidth of 40 kHz. The IF signal is amplified, the 100 Hz component is demodulated and amplified, and then the magnitude and phase of this Dicke-switch modulation component are measured in a phase sensitive detector. The phase detector output provides a dc error signal which is integrated (τ = 0.1 sec.) and then used to control the output level of the radiometer noise source. The noise source consists of a solid state noise diode and a high-gain, wideband amplifier. The amplifier gain can be varied over a 25-db

range; to increase the radiometer dynamic range to 65 db, three automatic range attenuators of 0-, 20-, and 40-db attenuation can be switched in at the noise source output. The noise source output required to match the antenna signal is measured using a precision thermistor bridge (τ = 0.5 sec.), and the thermistor bridge output is then telemetered to the ground. The integrated error signal in the servo loop is also telemetered to provide a redundant but somewhat less accurate measure of the antenna noise. The stability of the radiometers as measured by this error signal output has been better than $\pm$0.6 db over one year.

The Ryle-Vonberg radiometers used on the V antennas are connected via balun transformers which provide an approximate match to the antenna impedance. A pair of high-impedance preamplifiers connects the elements of the dipole antenna to the input balun for the dipole radiometer so as to minimize errors in the absolute measurements due to antenna reactance variation, inequalities in preamp impedances, and uncertainties in antenna radiation efficiency (Weber, 1968). The antenna temperatures due to cosmic noise in the RAE frequency range are $\gtrsim 10^6$ ^oK, consequently preamplifier noise temperatures of $\sim 10^3$ ^oK provide a good signal-to-noise ratio.

Fixed-frequency burst radiometers (BR's) are connected to the dipole and lower V antennas via high-impedance pre-amplifiers. The chief advantages of the BR's are high time resolution and relatively few components for high reliability. The BR is a simple total-power receiver consisting of an input balun, a power divider, and several parallel tuned-radio-frequency (TRF) strips. Each TRF strip is comprised of a bandpass filter having a bandwidth of 10% of the center frequency, an RF amplifier, and a detector. The total dynamic range of each channel is 60 db, and the detector time constant is 10 ms. The BR connected to the lower V antenna has eight independent frequency channels between 0.25 and 3.93 MHz. The dipole BR has six fixed-frequency channels between 0.54 and 2.80 MHz. Each frequency channel is sampled by the telemetry system twice a second. The BR connected to the dipole also contains a swept-frequency channel in which the frequency of a voltage-tuned filter is stepped through 32 channels between 0.2 and 5.4 MHz every eight seconds, and the filter output is amplified and detected as in the case of fixed-frequency BR channels. In this swept-frequency channel the bandwidth is 11% of the operating frequency and the time constant is 10 ms. Once every 10 minutes, during the experiment calibration cycle, a calibration noise source

is switched to the inputs of each preamplifier to provide a check on the long-term stability of each radiometer. The BR performance has proved to be very stable, and gain variations have been less than $\pm$0.3 db during more than two years of operation in orbit.

Every ten minutes during the experiment calibration cycle, the RAE impedance probe measures the complex impedance of both V antennas and an internal calibration load at nine frequencies between 0.24 and 7.86 MHz. The principle of operation of the impedance probe is illustrated in the block diagram in Figure 7. The reference oscillator applies a signal of 0.4 volts across the antenna via a wide-band balun. The test current into the antenna terminals is sensed by measuring the voltage drop across a resistor in series with the antenna. This current signal and the voltage across the antenna terminals are measured by two separate gain-stabilized amplifiers and mixed with the signal from a local oscillator to produce an IF in the range of 0.5 to 16 kHz. The IF products in each channel are then detected to produce an analog dc voltage proportional to the antenna voltage and current. The two IF signals are also put into a phase detector which develops a dc voltage related to the phase difference between the antenna voltage and current.

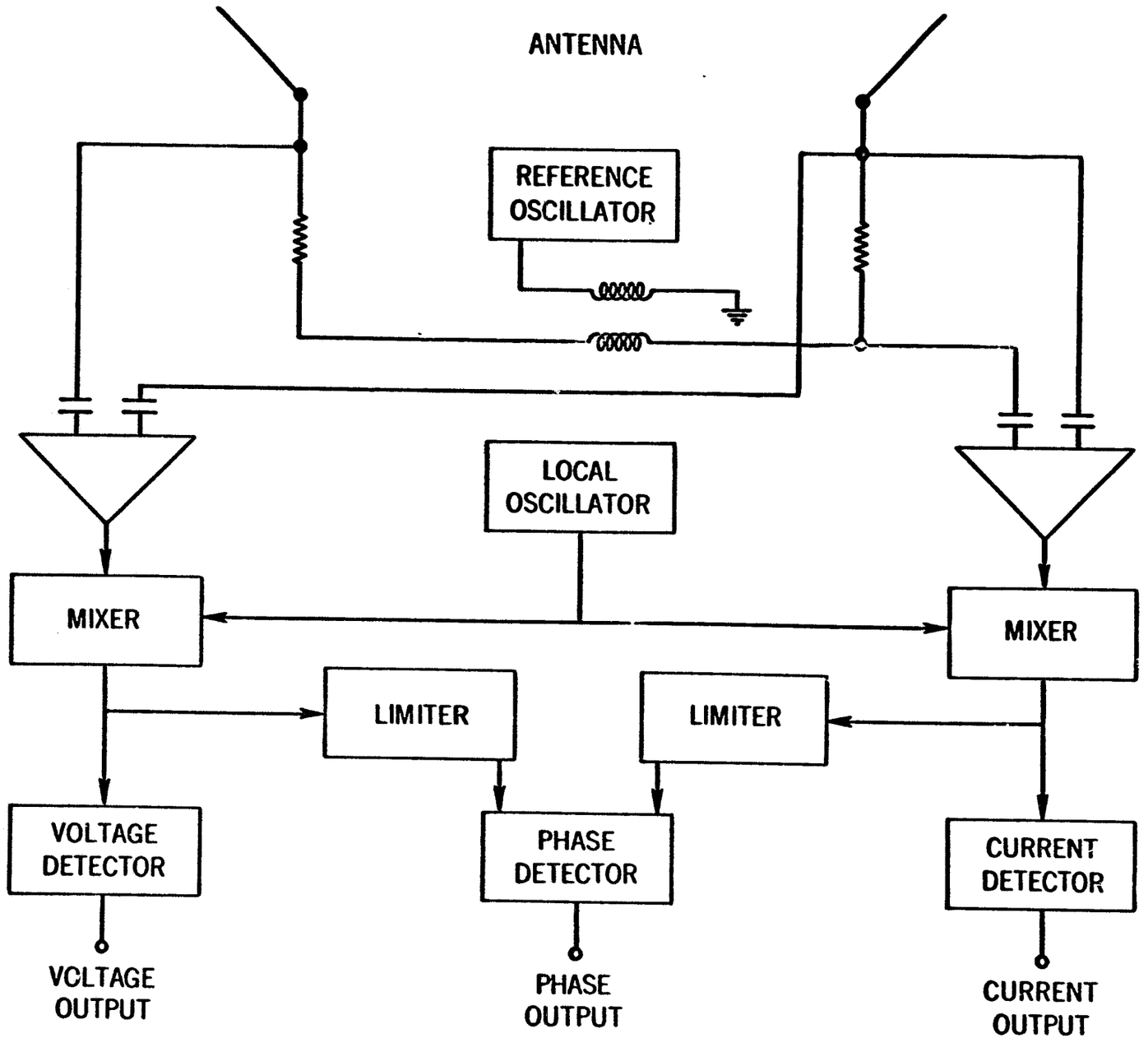

Figure 7. Simplified Block Diagram of V Antenna Impedance Probe.

The capacitance probe measures the dipole antenna capacitance in four frequency ranges centered at approximately 0.25, 0.70, 1.0, and 2.2 MHz. It finds the resonant frequency for a tuned LC circuit consisting of the dipole and one of four inductors available in the probe. Given the resonant frequency and the value of the inductor used, the output of the capacitance probe is readily translated into dipole capacitance. After accounting for uncertainties due to oscillator stability, the resonant frequency can be measured to 0.1%; this corresponds to sensitivity to capacitance changes of less than 1%. Once every 10 minutes during the same period that the antenna capacitance is measured, the probe is also switched to an internal calibration capacitor to provide a check on oscillator drift and any other system changes. Upon including uncertainties in the measurement of shunt capacitance due to the antenna deployment mechanism, errors in the probe calibration curves and uncertainties due to the effects of other spacecraft booms, the probable error in measurement of the dipole antenna capacitance in orbit is the order of $\pm$10%. A sample of two orbits of capacitance probe data at 0.9 MHz is shown in Figure 8 .

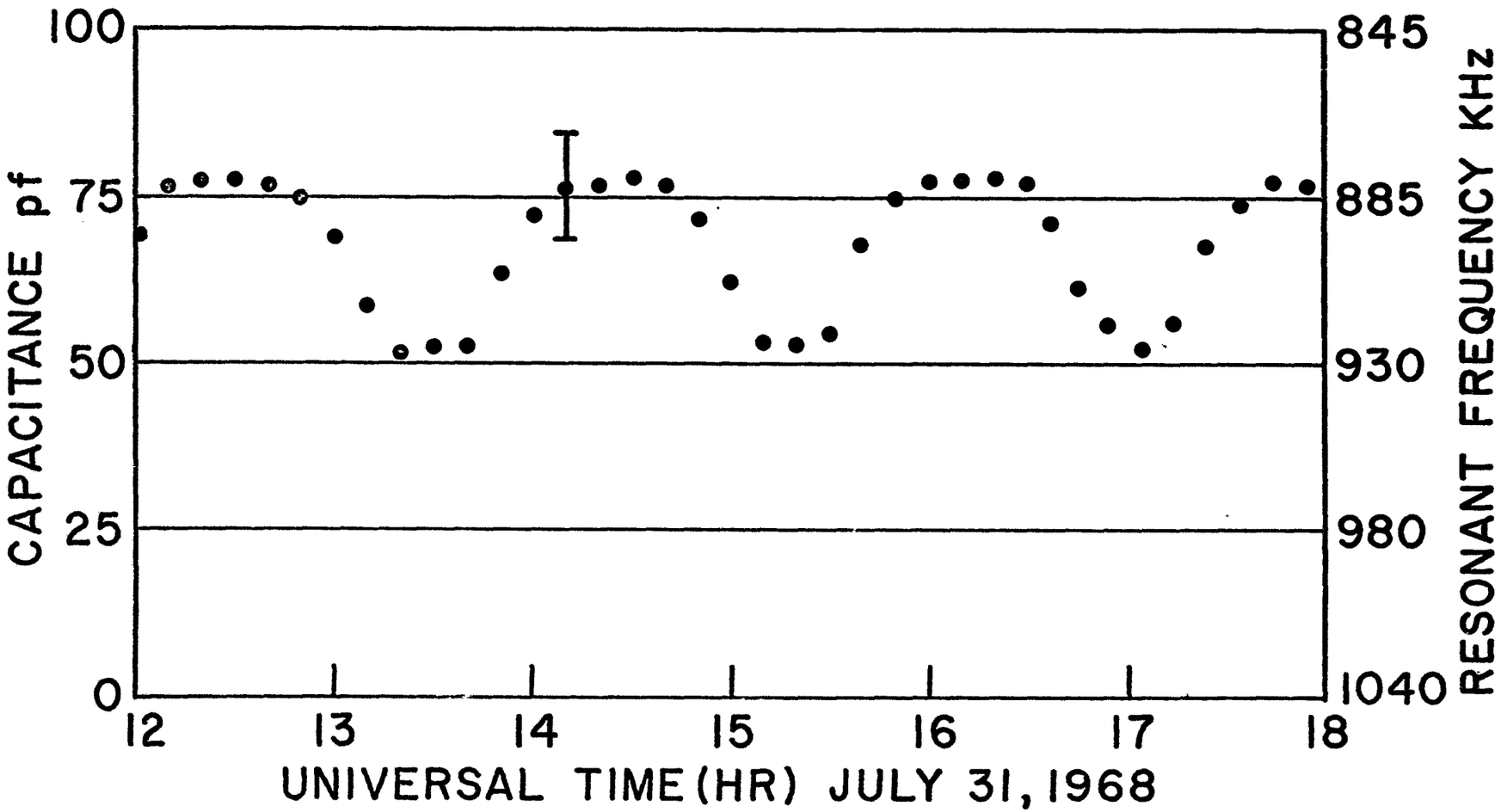

Fig. 8 - Dipole antenna capacitance data from the RAE capacitance probe. The minima at approximately 1330, 1520, and 1705 correspond to times when the satellite was in regions of relatively high electron density ($\sim 3 \times 10^3$ cm^{-3}) in the equatorial ionosphere.

V. CALIBRATION PROCEDURES

Great care was taken in the laboratory calibration of the radiometers and the impedance and capacitance probes. The final calibrations were performed using the flight cabling and telemetry system after the units were installed on RAE. In this manner, the actual flight configuration was most closely simulated. The calibrations were conducted at three spacecraft temperatures (-5^{o}, $+20^{o}$, and $+35^{o}$C) to cover the possible range of flight temperatures.

The primary noise standard was a temperature-limited noise diode having an absolute accuracy of $\pm$0.2 db. This noise source was used to calibrate a high-level noise generator ($T_{max} \sim 10^{14}\ ^{o}$K) by attenuating the high-level noise source to equal this standard. The resultant absolute accuracy in the secondary standard was $\pm$0.25 db when attenuator corrections were made. The stability of the high-level noise source was better than $\pm$0.01 db over a period of twelve hours.

The high-level noise source was connected to a transformer balun and two dummy antennas which simulated the flight antennas for noise calibration as shown in Figure 8. Calibration uncertainties arising from measurements of mismatch losses in the balun, dummy antennas, and transmission lines amounted to $\pm$0.3 db. Also shown in Figure 9 are a detector which monitored the noise level out of the attenuator, as

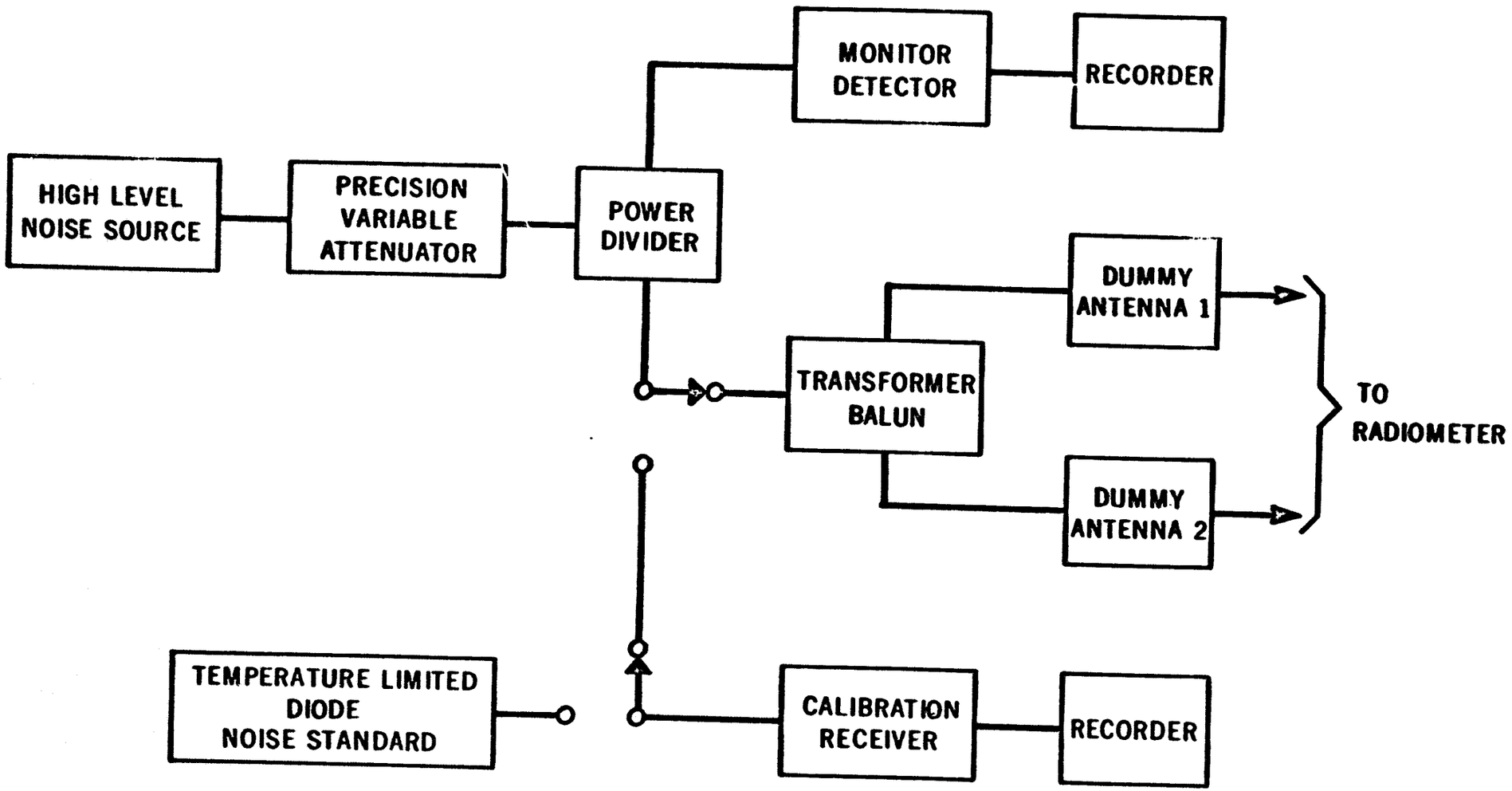

RAE RADIOMETER CALIBRATION DIAGRAM

Fig. 9 - RAE-1 radiometer calibration diagram.

well as the calibration receiver used to calibrate the high-level noise source against the standard. The RV and BR radiometers were calibrated in 1 db steps. The precision attenuators were stepped by a remotely controlled switching system which served to simplify calibration procedures but which introduced an uncertainty in the absolute insertion loss of the attenuator network of $\pm$0.2 db. The total uncertainty in absolute calibration of the radiometers including uncertainties in noise source absolute level, attenuator insertion loss, and losses in transmission lines and dummy antennas is estimated to be $\pm$0.44 db or $\pm$11%. These errors are summarized in Table 4.

In addition to noise calibration of the radiometers, their input impedance was measured at each operating frequency. The shunt capacitance and resistance of the antenna mechanisms were also measured and included in the analysis as part of the receiver impedance. This shunt impedance was maximized in the design of the antenna mechanisms in order to increase the effective radiometer input impedance. The shunt capacitance due to the 37-m dipole deployment mechanisms was about 7 pf. Since the mechanisms used for storing and extending the 229-m booms were much larger and more complicated, they introduced a shunt capacitance across the V antennas of the order of 83 pf.

TABLE 4. ABSOLUTE CALIBRATION OF RADIOMETERS

Absolute calibration of standard noise source.....	±0.2 db
Calibration of high level noise source against laboratory standard.....	±0.05
High level noise source stability	±0.01
Remotely controlled attenuator calibration	±0.2
Measurement of dummy antenna insertion loss	±0.15
Measurement of dummy antenna impedance	±0.3
probable error	±0.44 db

The impedance probe was calibrated on the spacecraft via many RL and RC loads. The loads were measured on impedance bridges to ±2% accuracy at each impedance probe operating frequency.

VI. DATA HANDLING METHODS

Every 9.86 minutes in orbit, RAE collects 16 independent readings at each of the nine frequencies on the Ryle-Vonberg radiometers on each antenna, 1152 samples on each of the 14 fixed-frequency burst radiometer channels, 72 swept radiometer scans, an impedance probe measurement at nine frequencies on each V antenna, a capacitance probe measurement at two frequencies on the dipole and a reading of some 80 performance parameters which monitor instrument voltages, temperatures and status. Telemetry data are either recorded in real time by tracking stations or stored on the spacecraft tape recorder for playback over selected stations at a speedup rate of 25:1. In this way, RAE data coverage was on the order of 95% during the first year in orbit and 90% during the second year.

The magnetic tapes containing the recorded RAE data are first checked for quality and edited when necessary. This is followed by separation of the various types of data from the telemetry format and rewriting onto separate tapes for each type. The output voltages from each experiment are

converted to useful engineering units via calibration curves stored in the computer. For the Ryle-Vonberg and burst radiometers, calibration curves of detector output voltage versus input noise temperature are stored in the computer in the form of a fifth degree polynomial fit to the pre-launch calibration data as illustrated in Figure 10. Samples of Ryle-Vonberg and BR data are shown in Figures 3 and 11. Spacecraft temperature corrections are made to the radiometer output by performing an interpolation between pre-launch calibration curves taken at three separate spacecraft temperatures. The resultant uncertainty in determining the radiometer input noise due to uncertainty in the calibration fit and radiometer temperature correction is $\pm$0.3 db. The uncertainty arising from the telemetry resolution is $\pm$0.2 db for the Ryle-Vonberg radiometers and $\pm$0.3 db for the burst radiometers. When combined with the uncertainties in the absolute calibration of the radiometers, the resultant uncertainty in determination of the absolute noise power at the radiometer inputs is approximately $\pm$0.6 db or $\pm$14%. For a 10% uncertainty in the free space impedance of the dipole antenna, our probable error in absolute antenna temperature measurements using the dipole radiometers is approximately $\pm$0.7 db or $\pm$18%.

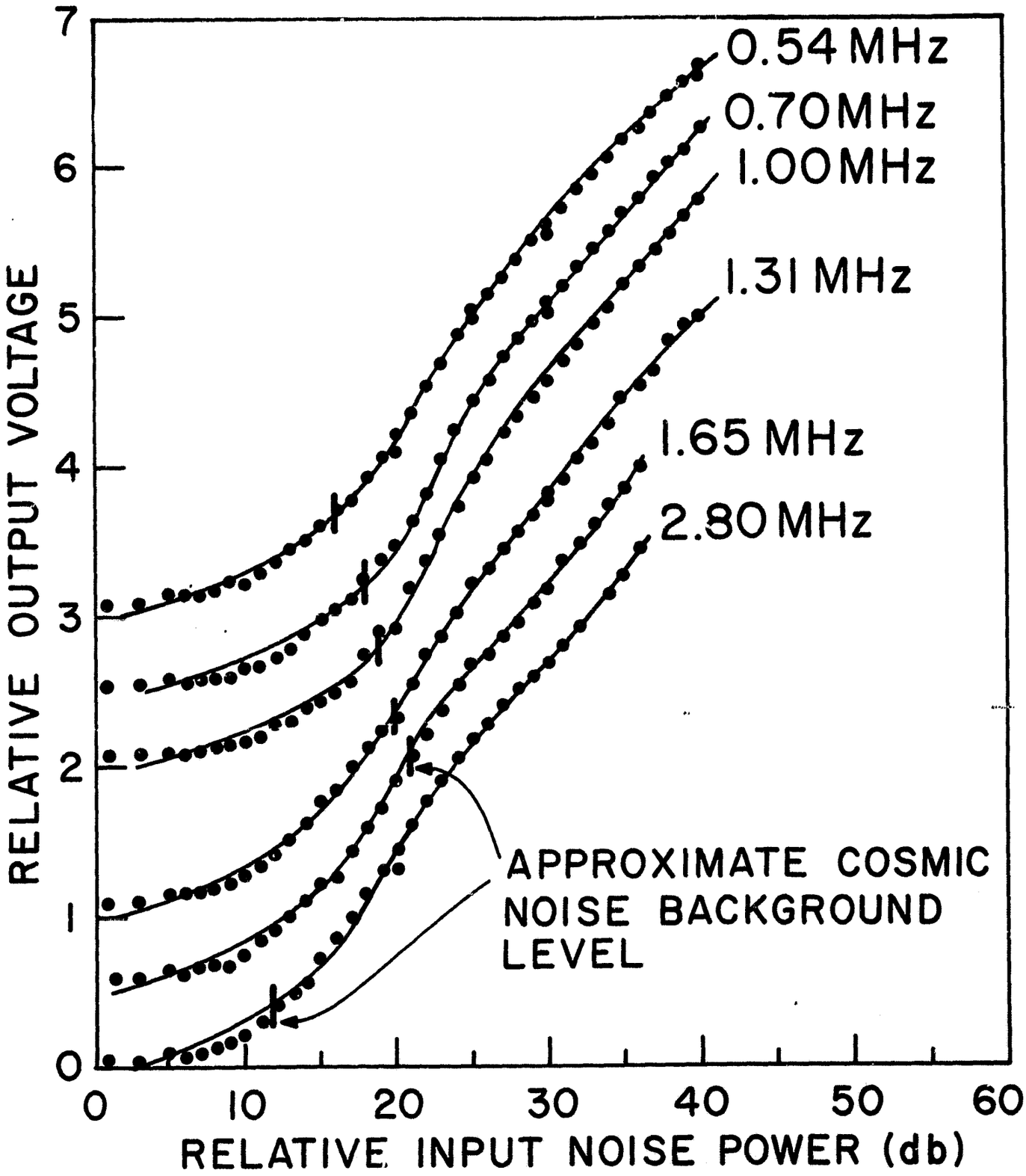

Fig. 10- Room temperature calibration curves for range 1 of the dipole burst radiometer. The dots denote the original calibration data; the smooth curves show the 5th degree polynomial computer fits. The curves have been displaced vertically for diplay purposes.

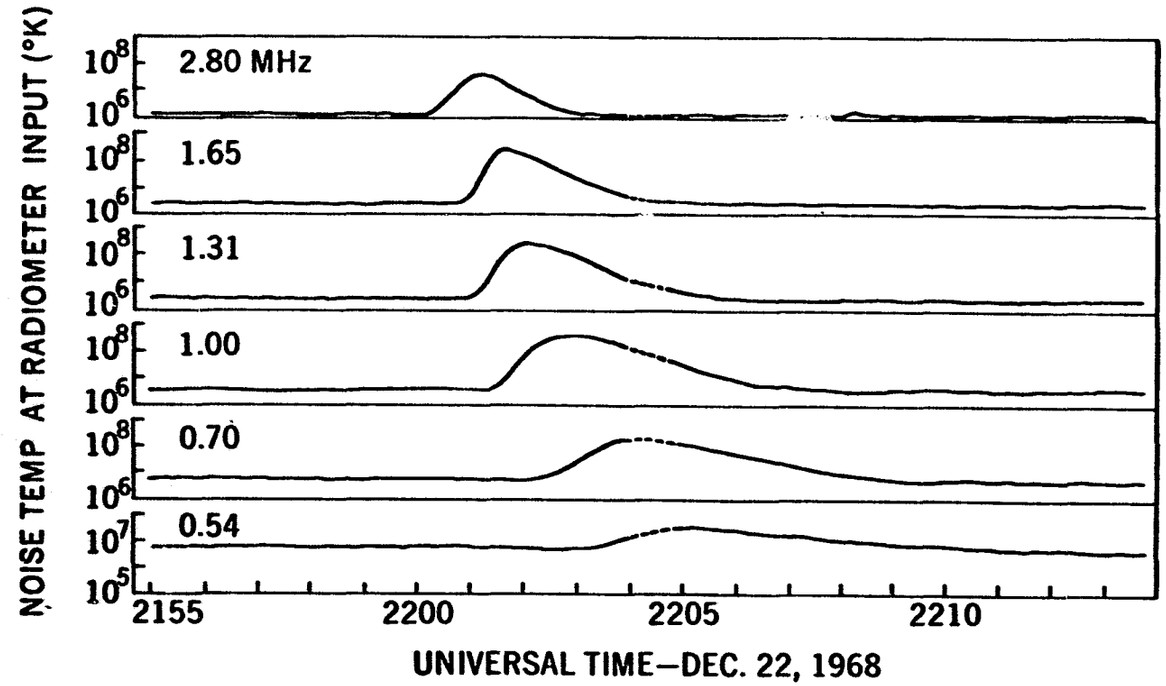

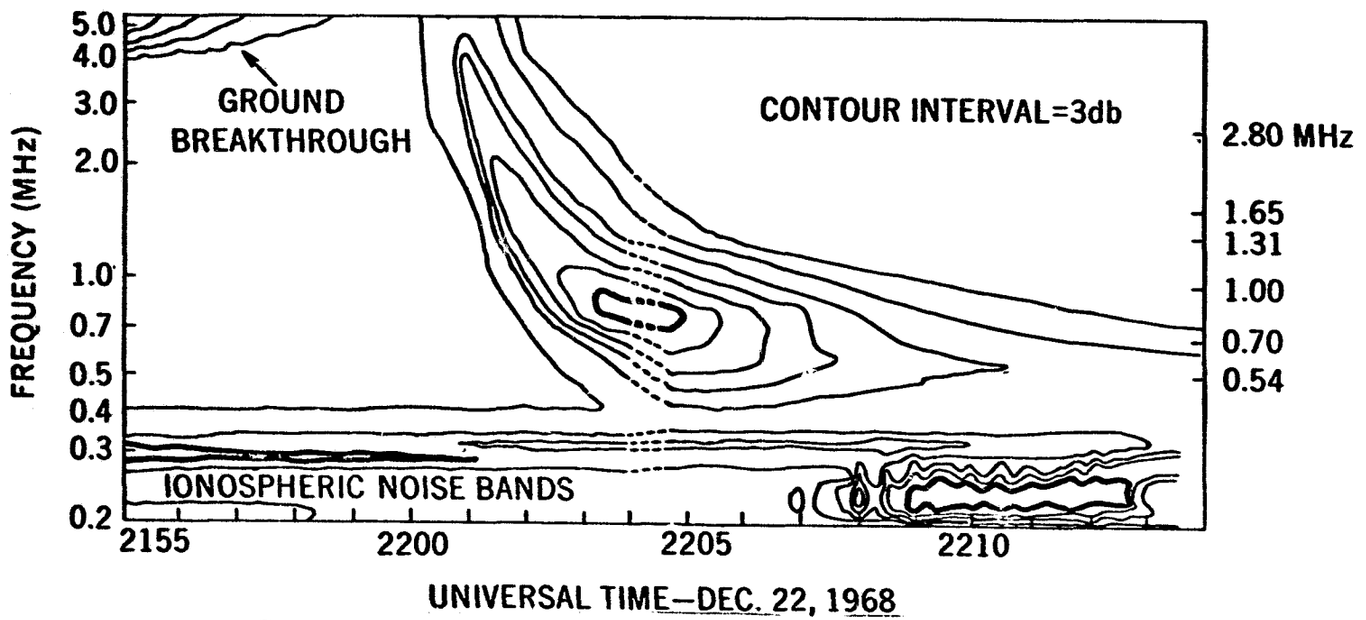

Fig. 11- Sample of data from RAE-1 dipole burst radiometer showing a type III solar radio burst. The dashed lines denote the time of an experiment calibration cycle.

VII. SYSTEM RELIABILITY

RAE-1 was designed for a one year minimum operating lifetime, and it has now been operating for nearly three years. Several failures have occurred on the spacecraft, none of which was considered major. The spacecraft tape recorder performance began to deteriorate after two months in orbit. Since that time the data have been received in real time, bypassing the tape recorder, resulting in minimal loss of data. The "fine" output channel of the Ryle-Vonberg radiometers failed after three to nine months of operation. These failures were traced to two reed relays in the thermistor bridge portion of each radiometer. The radiometer has been redesigned to replace these relays with solid state switches on future missions. The Ryle-Vonberg "coarse" output channels have provided good data without interruption, however. After about 18 months of operation, one of the preamplifiers on the lower V burst radiometer failed, reducing the sensitivity and changing the antenna pattern for that radiometer. The Ryle-Vonberg radiometer still operates on the lower V, so the BR failure is not a serious problem. After two years of operation in orbit the impedance probe locked on its internal calibration load due apparently to a relay failure, so no further V antenna impedance measurements are possible. In spite of these few cases of instrument malfunction, good data

are still being obtained on all three antenna systems.

VIII. EXPERIMENTAL RESULTS

Since the scientific results obtained with the RAE-1 are being presented elsewhere in the literature, we shall only summarize the major investigations that are being conducted. Using data from the dipole antenna, absolute spectra of the average cosmic noise background radiation have been obtained down to about 0.5 MHz with good continuity with ground-based measurements above 5 MHz (Alexander et al., 1969). These spectral measurements have been used to estimate the free-free absorption coefficient of thermal electrons and the synchrotron emissivity of low-energy cosmic ray electrons in the interstellar medium (Alexander et al., 1970) and to provide a new means of separating the galactic and extragalactic components of the background radiation (Clark et al., 1970). Two complete sky surveys for $|\delta| < 60^{o}$ have been completed using the upper V antenna. These data have not been completely reduced, however, since the job of accounting for antenna pattern effects, terrestrial and solar interference, etc. is both time consuming and complicated. When this analysis work is completed, we expect to produce several good maps of the distribution of the continuum background at frequencies in the 4-to-7 MHz range.

Investigations of solar radio bursts in the range of 0.2 to 5 MHz have been especially rewarding. Tens of thousands of type III bursts were observed in the first few months of the RAE lifetime (Fainberg and Stone, 1970). From an analysis of the type III burst drift rates it has been possible to estimate the burst exciter velocity, coronal electron density gradient, solar wind bulk velocity, and density inhomogeniety magnitude for active region coronal streamers in the altitude range of 10 to 40 $R_\odot$ (Fainberg and Stone, 1971). A second type of solar radio emission, hectometric continuum, has also been observed, and these results have been used to add to the understanding of the relationship of solar active regions, sources of continuum radio storms, and structure in the interplanetary medium.

In addition to the galactic background and the sun, another likely source of radio noise expected to be seen by RAE was the low frequency extension of the decameter wave radiation from Jupiter. The problem of detection and identification of sporadic noise bursts from Jupiter has proven to be far from simple due to the presence of numerous other sources of burst phenomena such as terrestrial, magnetospheric and solar noise. Using data from the time of a lunar occultation of Jupiter where no evidence for a disappearance or reappearance

was found in the dipole measurements, it has been possible to set an upper limit on the continuum flux from Jupiter between 0.5 and 5 MHz (Weber and Stone, 1970).

A wide variety of noise events that apparently originate in the terrestrial magnetosphere have been observed. These events, which can be so intense at times that all radiometer channels are saturated, are being studied to determine their relation to magnetospheric phenomena, regions of particle precipitation and ground breakthrough. Ionospheric noise bands generated in the frequency range between the upper hybrid resonance and the electron plasma cutoff are being studied to provide new information on the structure of the ionosphere at 6000 km. Using data from the dipole antenna capacitance probe, a picture of the variation of average electron density at 6000 km altitude as a function of local mean time and geomagnetic latitude has been derived.

IX. FUTURE PLANS

The second RAE spacecraft is presently scheduled for launch into an 1100-km altitude, lunar orbit in 1973. The basic experiment system will be identical to RAE-1. The lunar orbit, however, should have several significant advances over the capabilities of RAE-1. Interference from radio noise generated in the terrestrial magnetosphere which often appears in RAE-1 data should be reduced to an insignificant level much

of the time and eliminated entirely when the satellite is on the far side of the moon. Since the low-frequency limit for observations will be determined by the interplanetary plasma, the frequency range on the second RAE will be widened to 0.02-13 MHz. In addition to use of the 229-m V antennas for directive measurements, estimates of radio source positions may be obtained by utilizing the moon as an occulting disk. The lunar RAE data will also serve to improve our understanding of the radio frequency environment in the vicinity of the moon to support design efforts for future lunar observatories.

ACKNOWLEDGEMENT

The success of the RAE-1 is the result of the efforts of many scientisits, engineers, and technicians both in NASA and in private industry. Special thanks are due to the RAE Project Manager, John Shea, and to members of the Goddard Space Flight Center-Space Applications and Technology Directorate who designed and constructed the RAE and the Tracking and Data Systems Directorate who provided for the acquisition and processing of the RAE data. We also gratefully acknowledge the vital contributions of our colleagues L.W. Brown, T.A. Clark, J. Fainberg, R.J. Fitzenreiter, M.L. Kaiser and H.H. Malitson who have collaborated in the calibration and analysis of the RAE-1 experiments.

REFERENCES

Alexander, J.K., and Stone, R.G., (1964), A satellite system for radio astronomical measurements at low frequencies, Ann. d'Astrophys. 27, 837.

Alexander, J.K., Brown, L.W., Clark, T.A., Stone, R.G. and Weber, R.R., (1969), The spectrum of the cosmic radio background between 0.4 and 6.5 MHz, Astrophys. J. (Lett) 157, L163.

Alexander, J.K., Brown, L.W., Clark, T.A., and Stone, R.G., (1970), Low frequency cosmic noise observations of the constitution of the local system, Astro. & Astrophys. 6, 476.

Benediktov, E.A., Getmantsev, G.G., Mityakov, N.A., Rapoport, V.O., Sazonov, Yu., and Tarasov, A.F., (1965), Intensity measurements of radiation on frequencies 725 and 1525 kHz by means of receivers on the Electron 2 satellite, Cosmic Space Research: All-Union Conference on Space Physics (Moscow), 581.

Chapman, J.H., and Molozzi, A.R., (1961), Interpretation of cosmic noise measurements at 3.8 Mc/s from a satellite Nature 191, 480.

Clark, T.A., Brown, L.W., and Alexander, J.K., (1970), Spectrum of the extra-galactic background radiation at low radio frequencies, Nature 228, 847.

Duff, B.M., (1964), The resistively-loaded V-antenna; current distribution, impedance and terminal-zone correction, radiation field, Harvard Univ. Sci. Rept. NsG-579-3.

Ellis, G.R.A., Waterworth, M., and Bessell, M.S., (1962), Spectrum of the galactic radio emission between 10 Mc/s and 1.5 Mc/s, Nature 196, 1079.

Fainberg, J., and Stone, R.G., (1970), Type III solar radio burst storms observed at low frequencies. I: Storm morphology, Solar Phys. 15, 222.

Fainberg, J., and Stone, R.G., (1971), Type III solar radio burst storms observed at low frequencies. III: Streamer density, inhomogeniety, and solar wind speed, Solar Phys, 17, 392.

Getmantsev, G.G., Ginzburg, V.L. and Shklovskii, I.S., (1958), Radio astronomical investigations with the aid of artificial satellites, Uspekhi Fiz. Nauk 66, 157.

Haddock, F.T., (1960), Radio astronomy observations from space, Amer. Rocket Soc. J., 30, 598.

Hartz, T.R., (1964a), Observations of the galactic radio emission between 1.5 and 10 MHz from the Alouette satellite, Ann. d'Astrophys. 27, 823.

Hartz, T.R., (1964b), Solar noise observations from the Alouette satellite, Ann. d'Astrophys. 27, 831.

Huguenin, G.R., Lilley, A.E., McDonough, W.H., and Papagiannis, M.D., (1964), Measurements of radio noise at 0.7 and 2.2 Mc/s from a high altitude rocket probe, Planet. Space Sci. 12, 1157.

Huguenin, G.R., and Papagiannis, M.D., (1965), Spaceborne observations of radio noise from 0.7 to 7.0 MHz and their dependence on the terrestrial environment, Ann. d'Astrophys. 28, 239.

Iizuka, K., (1965), The traveling-wave V-antenna, Harvard Univ. Sci. Rept. No. NsG-579-4.

Iizuka, K., (1967), The traveling-wave V-antenna and related antennas, IEEE Trans. Ant. & Prop. AP-15, 236.

King, R.W.P., (1956), The Theory of Linear Antennas, Harvard Univ. Press (Cambridge) 190.

Lovell, A.C.B., (1959), Radio astronomical measurements from earth satellites, Proc. Roy. Soc. A 253, 494.

Sandler, S.S.,(1966), Radiation and current properties of the resistively loaded traveling-wave V-antenna, Northeastern Univ. Sci. Rept. No. NsG-355-3.

Schelkunoff, S.A., and Friis, H.T., (1952), Antennas, Theory and Practice, John Wiley and Sons (New York) 433.

Slysh, V.I., (1965), The measurement of cosmic radiation on frequencies 210 and 2200 kHz at heights to 8 earth radii on Zond 2, Kosmich. Issled. 3, 760.

Smith, F.G., (1964), Low frequency radio astronomical observations from rockets and satellites, Ann. d'Astrophys. 27, 819.

Smith, F.G., (1965), Cosmic radio noise as measured in the satellite Ariel 2; part II, analysis of the observed sky brightness, Mon. Not. Roy. Astro. Soc. 131, 145.

Somerlock, C.R., and Krustins, J., (1968), A precision spacecraft radiometer for hectometer wavelengths, NASA Tech. Note TN D-4634.

Tanner, R.L., and Andreasen, M.G., (1967), Numerical solution of electromagnetic problems, IEEE Spectrum 4, 53.

Walsh, D., Haddock, F.T., and Schulte, H.F., (1964), Cosmic radio intensities at 1.225 and 2.0 Mc/s measured up to an altitude of 1700 km, Space Research IV (ed. P. Muller), North Holland (Amsterdam) 935.

Weber, R.R., (1968), Design and calibration of low frequency radio astronomy space probes, Goddard Space Flt. Cntr. Rept X-615-68-73.

Weber, R.R., and Stone, R.G., (1970), Search for Jovian hectometric continuum radiation, Nature 227, 591.